J. Electrochem. Sci. Eng. **10(3)** (2020) 257-262; http://dx.doi.org/10.5599/jese.769

Open Access: ISSN 1847-9286
www.jESE-online.org

Original scientific paper

V_2O_5 as magnesium cathode material with extended cyclic stability

Charalampos Drosos[1,✉], Benjamin Moss[2], Andreas Kafizas[2,3,✉] and Dimitra Vernardou[4,✉]

[1]*Delta Nano – Engineering Solutions Ltd., Cyprus*
[2]*Department of Chemistry, Molecular Science Research Hub, Imperial College London, White City Campus, London, W12 0BZ, U.K.*
[3]*Grantham Institute for Climate Change, Imperial College London, South Kensington, London, SW7 2AZ, U.K.*
[4]*Department of Electrical & Computer Engineering, School of Engineering, Hellenic Mediterranean University, 710 04 Heraklion, Crete, Greece*

Corresponding authors: ✉info@delta-nano.com; ✉a.kafizas@imperial.ac.uk; ✉dvernardou@hmu.gr

Received: December 24, 2019; Revised: February 19, 2020; Accepted: February 22, 2020

Abstract

In this work, the electrochemical performance of aerosol-assisted chemical vapour deposited vanadium pentoxide cathodes at 600 °C, is presented. The as-grown oxides indicate specific discharge capacity of 300 mA h g^{-1} with capacity retention of 92 % after 10000 scans, coulombic efficiency of 100 %, noble structural stability and high reversibility. The present study shows the possibility to grow large-area magnesium cathode material with extended cycle stability via utilization of an aqueous electrolyte under a corrosive environment. This enhanced performance may be a combination of electrode morphology and adherence, when compared to previous work employing electrode growth temperature at 500 °C.

Keywords

Magnesium ion batteries; chemical vapor deposition; electrode morphology; coating adherence; corrosive environment.

Introduction

Aqueous metal-ion batteries (AIBs) are auspicious alternatives for large-scale energy storage since the water-based battery system is low cost, environmentally friendly, safe and does not require rigorous manufacturing conditions (elimination of glove box in the production line) [1]. Additionally, AIBs have no special operational and maintenance requirements and do not require regular charge because of low self-discharge [2].

In this perspective, multivalent-ion technologies (Mg^{2+}, Ca^{2+}, Al^{3+}) have been proposed as replacements for Li-ion technology because they can store more charge per ion at the cathode, leading to larger energy density than the univalent ion batteries [3]. Among them, magnesium-ion batteries have attracted attention due to the high abundance of magnesium (1.94 %) [4], high volume specific capacity (3833 mAh cm^{-3}) [5] and low reduction voltage (-2.37 V *vs.* SHE) [6].

In our previous work [7], the viability of a technology that is proven to be industrially competitive – that of cold-wall aerosol assisted chemical vapor deposition was established for the growth of vanadium pentoxide (V_2O_5) with excellent performance as cathodes for aqueous magnesium-ion batteries (specific discharge capacity 427 mA h g^{-1} with capacity retention of 82 % after 2000 scans). The cathodes presented an increase of current intensity as the scan number proceeded to 500, remaining however unchanged after 1000 scans. Inspired by the respectable results of Mg^{2+} ion battery chemistry, herein we would like to report that this path can be further exploited and enhanced for high-performance cathode materials. In this work, we demonstrate that a mixed phase of α-V_2O_5 and β-V_2O_5 deposited at 600 °C (*i.e*. higher substrate temperature than before [7]) is capable of reversibly inserting magnesium ions showing a specific discharge capacity of 300 mAh g^{-1} with capacity retention of 92 % after 10000 scans, which may be a combination of electrode morphology and adherence. This particular cathode offers a safe and economical energy storage solution to large-scale applications with extended cyclic stability.

Experimental

Synthesis of V_2O_5 cathodes

Thin layers of V_2O_5 were deposited at 600 °C, following the same procedure of aerosol-assisted chemical vapor deposition (AACVD) as previously published [7], having similar characteristics in color and stability.

Physical characterization

X-ray diffraction (XRD) was implemented to study the structure of V_2O_5 coatings on a modified Bruker-Axs D8 diffractometer. Field-emission scanning electron microscopy (FE-SEM) and x-ray photoelectron spectroscopy (XPS) were utilized to evaluate the surface morphology and chemistry of the material in its initial state, after Mg^{2+}intercalation and 10000 continuous Mg^{2+} intercalation/deintercalation scans. The processing parameters and the instruments employed were the same as those reported in [7].

Electrochemical performance

The AACVD coating, Pt foil (with surface area 1 cm^2) and Ag/AgCl/KCl (0.1 M) were acted as working, counter and reference electrodes [7,8], respectively. An aqueous solution of 0.075 M $MgCl_2$ was conducted as the electrolyte in all measurements for the scan rate of 10 mV s^{-1} and potential ranging -1.5 V to +1.0 V. Cyclic voltammograms, potentiometric measurements and electrochemical impedance spectroscopy (EIS) studies were performed in an electrochemical workstation (PGSTAT302N) [7].In particular, EIS curves were performed for alternating current (AC) amplitude of 5.0 mV and set potential of -1.0 V over the frequency range of 100 kHz - 10 mHz.

Results and discussion

The crystal structure of the coating presents three peaks at 12.6, 21 and 30.7^o with respective Miller indices (200), (001) and (301) (Figure 1a). The first one is consistent with the formation of β-V_2O_5 [9],

while the other two with α-V_2O_5[10]. Regarding the rest of the peaks (■) are due to the FTO glass substrate [11]. To further investigate the surface chemistry, XPS indicates in Figure 1b binding energies at 517.3 (V $2p_{3/2}$), 524.9 (V $2p_{1/2}$) and 530.2 eV (O 1s), which correspond to V^{5+} and O^{2-} of V_2O_5 [12,13]. Additionally, there is a peak at 532.6 eV associated with the presence of chemisorbed OH groups on the surface of the coating [12]. Increasing the substrate temperature from 500 °C [7] to 600 °C, leads to the improvement in the crystallinity (*i.e.* (001) peak intensity increases) as expected for a conventional activated process. Higher temperatures enhance surface mobility, which in turn improves coating crystallization. The co-existence of α- and β-V_2O_5 is supported by SEM analysis indicating the grain structure recorded at magnification of ×50k (inset of Fig. 1a). It is clearly observed that the coating exhibits a compact structure with well distributed grains as compared with pure α-V_2O_5 [7]. The grains have irregular shape presenting some degree of agglomeration.

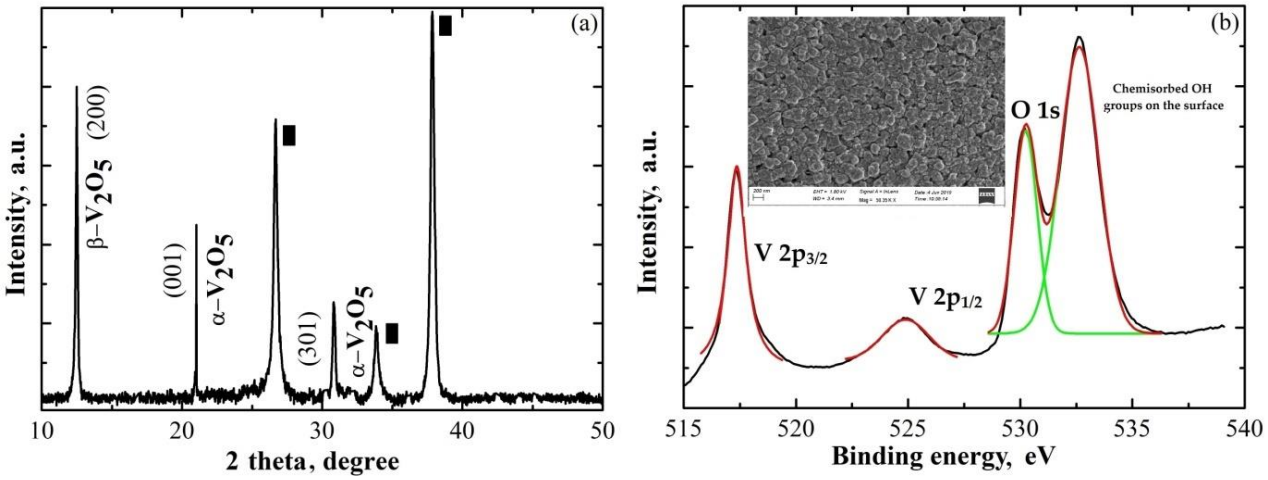

Figure 1.*XRD of V_2O_5 coating grown on FTO glass substrate by AACVD at 600 °C (squares represent reflections from FTO glass substrate) (a). XPS depth profile and FE-SEM image at ×50000 of V_2O_5 coating as inset (b).*

The electrochemical intercalation of Mg^{2+} into V_2O_5 coatings was studied in a three-electrode electrochemical cell using an aqueous solution of 0.075 M $MgCl_2$ as electrolyte. To examine if Mg^{2+} ions intercalate into the lattice of the host material, the state of the vanadium was examined by XPS. Figure 2a inset shows Mg 1s spectrum, which presents one peak at 1304 eV [14].

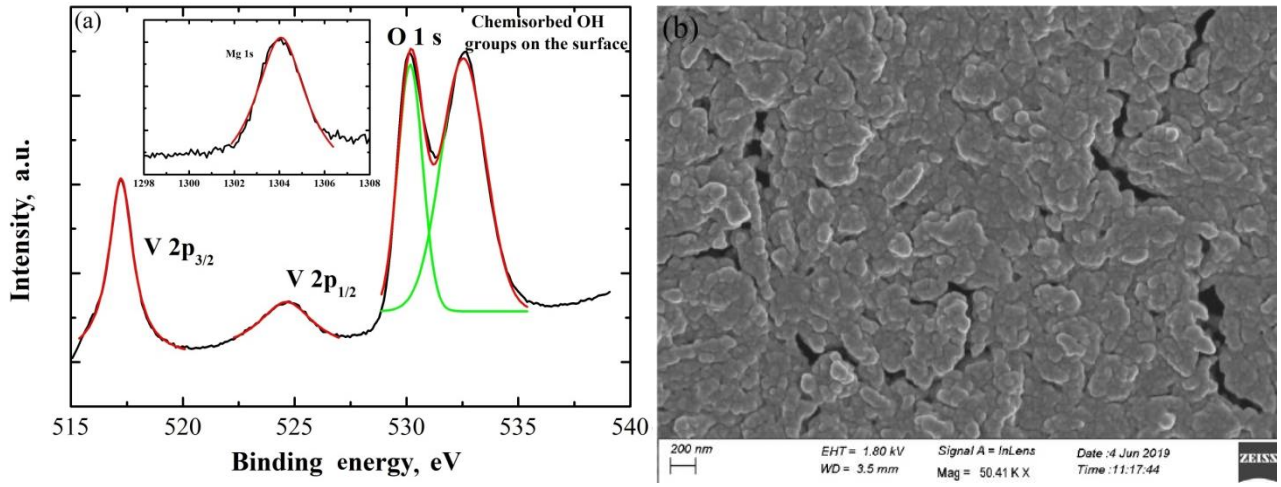

Figure 2. *XPS depth profiles **(a)** and FE-SEM image **(b)** at ×50000 after Mg^{2+} intercalation into the host of V_2O_5 coating.*

The clear magnesium signal indicates that metallic Mg is indeed intercalated from the electrolyte. The core level XPS spectrum of O 1s indicates two peaks, which are located at 530.1 and 532.5 eV due to O^{2-} in V_2O_5 and OH groups on the surface of V_2O_5 [12], respectively. After Mg^{2+} intercalation in the host of V_2O_5, the XPS spectrum resembles that of V_2O_5 in Figure 1a and only minor morphological changes observed (Figure 2b). The stability of V_2O_5 was evaluated *via* cyclic voltammograms for 10000 continuous Mg^{2+} intercalation/deintercalation scans (Figure 3a) in the aqueous $MgCl_2$ 0.075 M electrolyte sweeping the potential from -1.5 V to +1.0 V (*vs.* Ag/AgCl/KCl(0.1 M)). The voltammograms show one oxidation peak at -0.61 V with the reverse reaction occurring, as presented by the corresponding reduction peak at -1.10 V. These peaks are observed after the first scan due to the activation of intercalation/deintercalation processes into V_2O_5 host cathode material. The current density was found to decrease from the first to the 2000th scan and remained constant afterwards, presenting an extended cyclic stability compared to the previously published work [7].

The specific capacity of V_2O_5 cathode was evaluated under the constant specific current of 15 A g^{-1} and applied potentials ranging from -1.5 V to +0.7 V for the first and the 10000th scan (Figure 3b). A peak at approximately -1.12 V is indicated, employing the one-step deintercalation (discharge) process for the specific current applied. Additionally, a faint plateau is shown at approximately +0.5 V suggesting the one-step intercalation (charge) process. The specific discharge capacity was estimated to be 300 mA h g^{-1} with capacity retention of 92 % after 10000 scans and coulombic efficiency of 100 %. The capacity performance of this electrode is enhanced as compared to AACVD V_2O_5 at 500 °C [7], $FeVO_4$ in 1 M Mg SO_4 (300 mA h g^{-1}, efficiency: 100 % after 50 cycles [15]) and magnesium manganese oxide sieves in 0.5 M $MgCl_2$ (300 mA h g^{-1}, efficiency: 100 % after 300 cycles [16]). Finally, the shape of the curves remained unchanged for the first to the 10000th proposing good electrode stability.

Rate capability of the electrodes was studied at specific currents of 3.9 A g^{-1} up to 15 A g^{-1}, and then returned to 15 A g^{-1} (Figure 3 c). The electrode shows the highest specific discharge capacity at 15 A g^{-1} (300 mA h g^{-1}), which could still deliver the same value when the specific current returned to 15 A g^{-1} exhibiting capacity retention of 100 %. This performance confirms the upright structural stability and high reversibility of the cathode. The specific discharge capacity shows a rising trend with increasing specific currents, which is similar with the AACVD V_2O_5 at 500 °C [7].

Impedance responses of AACVD V_2O_5 cathode were evaluated by Nyquist plots for 1, 4000 and 8000 scans (Figure 3d). The experimental data were fitted by the electrical equivalent circuit (EEC) shown in Figure 3d inset. EEC consists of two parallel R-C circuits in series, for which a discussion still exists on the attribution of different elements to different processes in intercalation battery electrodes. Here, R_1 is ascribed to the electrolyte and FTO resistances, R_2 to the contact resistance between FTO and V_2O_5, which could possibly be influenced with artefacts due to presence of CE and RE in three-electrode cell, and R_3 to the charge transfer reaction resistance at V_2O_5/redox electrolyte interface [17,18].The first semi-circle (high-frequency) slightly changes upon different scan numbers, while the second semi-circle (low-frequency)is larger from the first to the 8000th scan showing however the percentage increase is smaller after 4000 scans (26 %). The impedance shape of the curves is not the same with those reported in [7] due to the differentiation of materials structure and morphology at higher growth temperature.

Ragone plot is used to relate the power density with the energy density using the total weight of the active material (0.0028 g), the cell voltage and the capacity based on charge/discharge curves at various current densities. The vanadium pentoxide cathode achieved a high value of 448 Wh kg^{-1} at 24200 W kg^{-1}. Assuming that the cathode takes up 50 wt.% of a cell, the magnesium-ion cell with

V_2O_5 cathode can deliver a 224 W h kg^{-1}, which is comparable with Li-ion batteries (<300 W h kg^{-1}_{cell}) and Li-S batteries (<500 W h kg^{-1}_{cell}) [19].

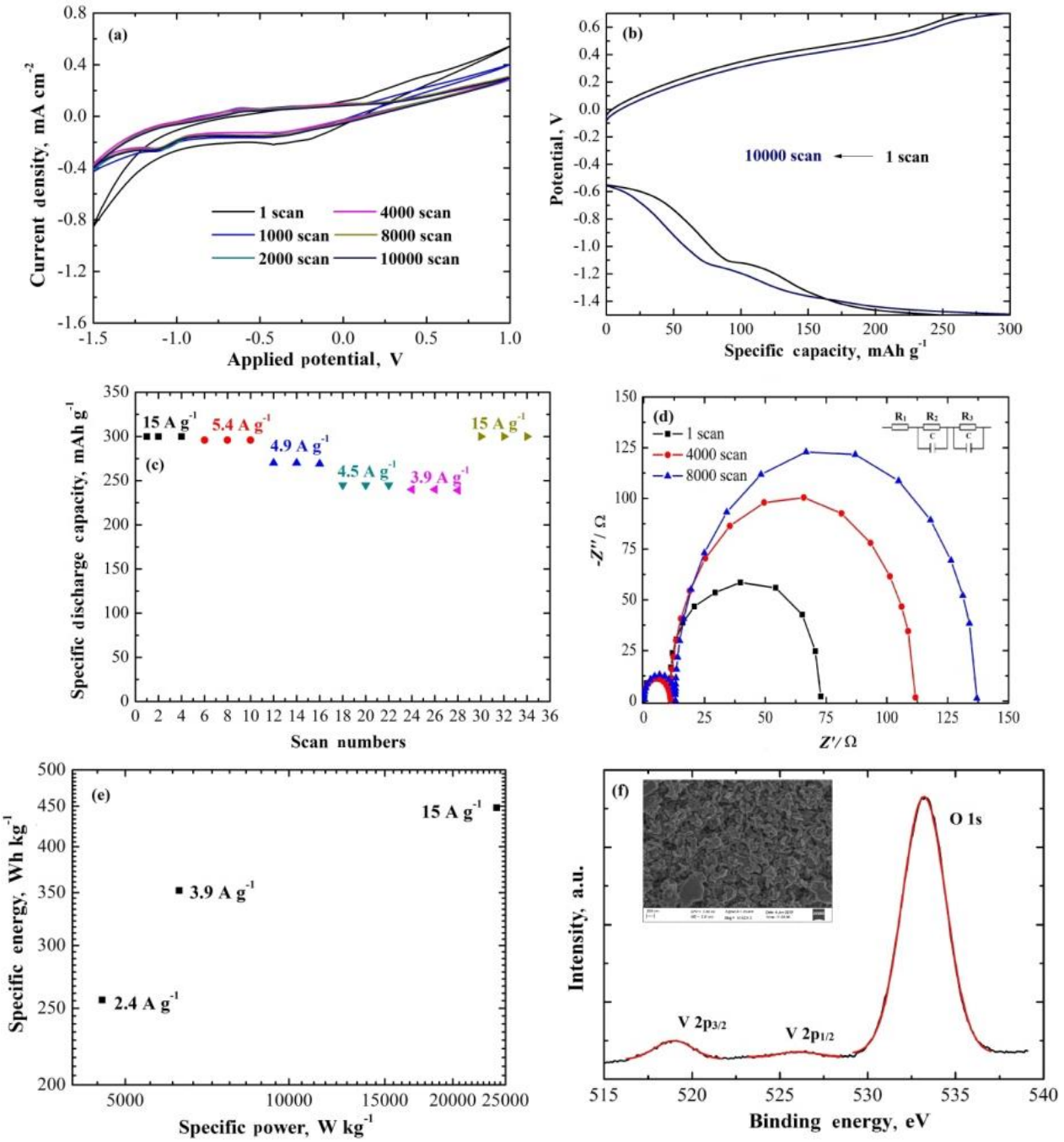

Figure 3. *Cyclic voltammetry curves of AACVD V_2O_5 for 1, 1000, 2000, 4000, 8000 and 10000 scans in 0.075 M $MgCl_2$ at scan rate of 10 mV s^{-1}(a). Specific capacity for V_2O_5 cathode for a potential ranging -1.5 V to +0.7 V under constant specific current of 15 A g^{-1} for 1 and 10000 scans (b).Rate capability of the electrode at specific current values of 3.9 A g^{-1} up to 15 A g^{-1} and then back to 15 A g^{-1}(c). Nyquist plot of measured (symbols) and fitted (solid lines) of V_2O_5 electrode after 1, 4000 and 8000 scans. Electrical equivalent circuit is also indicated as inset (d). Ragone plot based on the mass of the active material, cell voltage and capacity values obtained in Figure 3b (e). XPS depth profiles and FE-SEM image at ×50000 of V_2O_5 as inset, after 10000 continuous Mg^{2+} intercalation/deintercalation scans (f)*

Finally, the surface morphology and chemistry of V_2O_5 cathodes were studied after 10000 continuous intercalation/deintercalation scans. The grains appear elongated due to changes associated with Mg^{2+} intercalation/deintercalation processes in V_2O_5 (Figure 3f, inset). The presence of V_2O_5 is

still supported after 10000 scans (Figure 3f) with lower intensity as compared with Figure 1b), whereas the peak due to chemisorbed OH groups at 532.6 eV disappears upon cycling due to the weak interaction of water with the metal oxide.

Conclusions

This paper demonstrates the utilization of cold-wall AACVD to grow V_2O_5 electrodes as cathodes for magnesium ion batteries. Furthermore, the growth temperature increase to 600 from 500 °C (reported previously) is found decisive forV_2O_5 cathode with extended cyclic life. This enhancement may be a combination of the co-existence α- and β-V_2O_5 along with the adherence of the coating. In particular, the electrode indicated a specific discharge capacity of 300 mA h g^{-1} with capacity retention of 92 %, coulombic efficiency of 100 %, good structural stability and comparable specific energy values with Li-ion and Li-S batteries under a corrosive environment. This was obtained for the first time to the best of our knowledge.

References

[1] H. Ao, Y. Zhao, J. Zhou, W. Cai, X. Zhang, Y. Zhu, Y. Qian, *Journal of Materials Chemistry A* **7** (2019) 18708-18734.
[2] J. F. Whitacre, T. Wiley, S. Shanbhag, Y. Wenzhuo, A. Mohamed, S. E. Chun, E. Weber, D. Blackwood, E. Lynch-Bell, J. Gulakowski, C. Smith, D. Humphreys, *Journal of Power Sources* **213** (2012) 255-264.
[3] J. L. Andrews, A. Mukherjee, H. DeogYoo, A. Parija,P. M. Marley, S. Fakra, D. Prendergast, J. Cabana, R. F. Klie, S. Banerjee, *Chem* **4** (2018) 564-585.
[4] J. O. Besenhard, M. Winter, *ChemPhysChem* **3** (2002) 155-159.
[5] M. Matsui, *Journal of Power Sources*, **196** (2011) 7048-7055.
[6] R. Attias, M. Salama, B. Hirsch, Y. Gofer, D. Aurbach, *ChemElectroChem* **5** (2018) 3514-3524.
[7] C. Drosos, C. Jia, S. Mathew, R. G. Palgrave, B. Moss,A. Kafizas, D. Vernardou, *Journal of Power Sources* **384** (2018) 355-359.
[8] D. Vernardou, M. Apostolopoulou, D. Louloudakis, N. Katsarakis, E. Koudoumas, *Journal of Colloid and Interface Science* **424** (2014) 1-6.
[9] B. Saravanakumar, C. Selvam,G. Ravi, M. Thambidurai, R. Yuvakkumar, *AIP Conference Proceedings* **1992** (2018) 040028.
[10] Y.-H. Zhu,Q. Zhang,X. Yang,E.-Y. Zhao,T. Sun,X.-B. Zhang,S. Wang, X.-Q. Yu,J.-M. Yan, Q. Jiang, *Chem* **5** (2019) 168-179.
[11] M. Lv, D. Zheng, M. Ye, L. Sun, J. Xiao, W. Guo, C. Lin, *Nanoscale* **4** (2012) 5872-5879.
[12] S.Tepavcevic, Y. Liu,D. Zhou, B. Lai, J. Maser, X. Zuo,H. Chan,P. Král,C. S. Johnson, V. Stamenkovic, N. M. Markovic,T. Rajh, *ACS Nano* **9** (2015) 8194-8205.
[13] Z. Xie, J. Lai, X.Zhu,Y. Wang, *ACS Applied Energy Materials* **111** (2018) 6401-6408.
[14] H. Zhang, K. Ye, X. Huang, X. Wang, K. Cheng, X. Xiao, G. Wang, D. Cao, *Journal of PowerSources* **338** (2017) 136-144.
[15] H. Zhang, K. Ye, K. Zhu, R. Cang, J. Yan, K. Cheng, G. Wang,D. Cao, *Chemistry-A European Journal* **23** (2017) 17118-17126.
[16] H. Zhang, K. Ye, S. Shao, X. Wang, K. Cheng, X. Xiao, G. Wang, D. Cao, *Electrochimica Acta* **229** (2017) 371-379.
[17] G. Niu, W. Li, F. Meng, L. Wang, H. Dong and Y. Qiu, *Journal of Materials Chemistry A* **2** (2014) 705-710.
[18] J. Park, J. Woo Choi, W. Kim, R. Lee, H. Chul Woo, J. Shin, H. Kim, Y. Jun Son, J. Young Jo, H. Lee, S. Kwon, C. -L. Lee, G. Young Jung, *RSC Advances* **9** (2019) 14868-14875.
[19] P. G. Bruce, S. A. Freunberger, L. J. Hardwick, J.-M. Tarascon, *Nature Materials* **11** (2012) 19-29.